Semiconductor Electrodes

XI. Behavior of n- and p-Type Single Crystal Semconductors Covered with Thin n-TiO₂ Films

Paul A. Kohl,* Steven N. Frank,** and Allen J. Bard**

Department of Chemistry, The University of Texas at Austin, Austin, Texas 78712

ABSTRACT

Single crystal semiconductors (n-Si, p-Si, n-GaAs, p-GaAs, n-GaP, n-InP, and n-CdS) were coated with n-type TiO₂ by a chemical vapor deposition technique, and the electron and hole transfer properties across the heterojunction so produced were investigated. The quality of the deposited TiO₂ film depended upon several factors including temperature and substrate material. When high quality crack-free TiO₂ coats were obtained on n-type substrates, the substrate was stabilized with no dissolution during the photo-oxidation of water. However, the oxidation was due only to the photoexcitation of the TiO₂, and any holes produced in the substrate were not transferred through the TiO₂ to the solution. The use of p-type substrates coated with TiO₂ as photocathodes was limited by band-bending requirements at the p-n heterojunction and the TiO₂-solution interface.

The utilization of small bandgap (E_g) semiconductor electrodes, i.e., $E_g < 2.5$ eV, such as CdS, Si, and GaAs, for the efficient conversion of solar energy to electrical or chemical energy in electrochemical cells is limited by the dissolution or decomposition of the semiconductor itself (1). Photoeffects and the electrochemical behavior of semiconductor electrodes have been described elsewhere [see, e.g., (2-4) and references therein]. Various attempts have been made to stabilize the surface of small bandgap semiconductors without changing their electrochemical properties for hole or electron transfer through the electrode-solution interface. For example, thin metal films have been deposited on the surface of the semiconductor (5) or different redox couples (e.g., Na₂S/S with CdS) have been added to the solution to allow a preferential electrode reaction rather than the dissolution of the semiconductor (6-9). N-type TiO₂, SnO₂, and SrTiO₃ show sufficient stability so as not to decompose during the photo-oxidation of water (10-12). However, these have bandgaps ≥ 3.0 eV so that they utilize only a very small percentage of the solar spectrum.

There has recently been some interest in using chemically vapor deposited coatings on semiconductor electrodes. For example, CVD TiO₂ coats on n-CdS have been reported (13) to increase its efficiency as a photoanode and decrease the dissolution of the CdS. Other work in this area (14) indicates that n-GaP with TiO₂ coatings stabilize the GaP against photodissolution at potentials positive of the flatband. The heterojunction produced at the interface of the two dissimilar semiconductors creates an energy barrier to the transfer of carriers across the junctions with a magnitude determined by the relative position of the conduction and valence bands, as shown in the discussion following. This barrier would be expected to hinder the flow of photogenerated carriers from the substrate through the protective coating. However, energy levels and surface states may exist in the bandgap region and be utilized for electron transfer reactions, e.g., an intermediate level has been proposed for TiO₂ (6). If these levels extend into the semiconductor and can be considered "bandlike," the possibility exists for the transfer of electrons and holes through the coating via these intermediate levels.

In this work, various small bandgap semiconductors (n-Si, p-Si, n-CdS, n-GaAs, p-GaAs, n-GaP, and n-InP)

were coated with polycrystalline TiO₂ by chemical vapor deposition (CVD) to examine the resulting electrical properties both with and without a solution interface. The position of the valence and conductions bands vs. vacuum for the various semiconductors is shown in Fig. 1 (15, 16). The procedure for obtaining a good TiO₂ film on small bandgap single crystal semiconductors, a modification of the one previously described (17), the electrode properties, and the conditions by which photoexcited electrons or holes are transferred from the substrate to the solution via the large bandgap TiO₂ film on the surface are reported.

Experimental

The low resistivity single crystal semiconductors used as substrates for chemical vapor deposition of polycrystalline TiO₂ were about 1 mm thick and were polished with 0.5 μm alumina. The CVD, with the apparatus described previously (17), was done at various substrate temperatures (100°-600°C) to find the optimum temperature for a good quality TiO₂ film. The annealing process was performed either on a hot plate
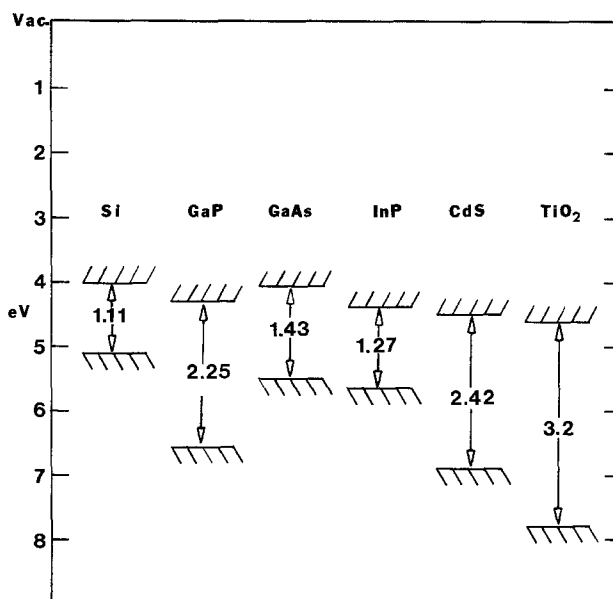

Fig. 1. Relative position of the valence and conduction bands vs. vacuum of the various semiconductors used.

225

at 600°C or under high vacuum at 700°C; the flame method used previously was not employed here because of the easy oxidation of most semiconductor materials at flame temperatures in the presence of oxygen. The n-type TiO₂ was reduced to increase its conductivity by passing hydrogen gas over the heated sample or by heating in a high vacuum.

The n-GaP, n-GaAs, and p-GaAs were obtained from Atomergic Chemicals (Long Island, New York). The n-Si and p-Si crystals were donated through the courtesy of Texas Instruments (Dallas, Texas), and the n-CdS and n-InP were originally obtained from National Lead and donated by Dr. D. I. Tchernev (Lincoln Laboratories, Massachusetts Institute of Technology). Ohmic contacts were made to the n-CdS, n-InP, and n-GaP by electroplating indium on the back side of the crystals using a 0.1M InCl₃ solution. The n-GaP contact was heated in a hydrogen atmosphere at about 400°C for several hours to make it ohmic. Ohmic contacts were obtained with p-GaAs and p-Si (3) by electroplating gold from a 0.1M Au(CN)₂⁻ solution on the rear side. Contact to n-Si (3) was made by electroplating nickel from a 0.1M Ni(NO₃)₂ solution and to n-GaAs (18) by first plating indium, then gold, and alloying at 400°C in a hydrogen atmosphere. To confirm that the contacts were ohmic, a second contact was made to the rear side; in all cases of good contacts the resistance between the contacts was small and the current was directly proportional to the applied potential independent of polarity. A wire was connected to the ohmic contact with conducting silver epoxy (Allied Products Corporation, New Haven, Connecticut). The back and sides of the crystal were then sealed with nonconducting 5 min epoxy (Devcon Corporation, Danvers, Massachusetts). The crystals were then mounted on a small glass disk connected to a glass tube with silicone adhesive (Dow Corning, Midland, Michigan) which allowed a path for the wire. When an ohmic contact was made on the front side of the crystal on the TiO₂, it was accomplished with silver epoxy and the contacts insulated as described above. Duplicate semiconductor electrodes were prepared in an identical manner except without the TiO₂ film for comparison with the filmed electrodes.

All chemicals were reagent grade and all solutions were prepared with triply distilled water, with the first distillation from alkaline potassium permanganate.

A three-compartment cell, similar to previous designs (6), was used for all electrochemical measurements. The reference compartment made electrical contact with the main compartment via a porous Vycor glass junction. The counterelectrode was a platinum wire and the reference electrode was a silver wire in 0.1M AgNO₃. However, all values are reported *vs.* a saturated calomel electrode (SCE). The main compartment had an optically flat Pyrex window.

A PAR 173 potentiostat and PAR 175 universal programmer (Princeton Applied Research Corporation, Princeton, New Jersey) were used. Data were recorded on a Houston Instruments Model 2000 X-Y recorder. For photoexcitation experiments, a 450W xenon lamp and grating monochromator (Oriel Corporation, Stamford, Connecticut) were used. The electron micrographs were taken with a scanning electron microscope (SEM) JSM-2 (Japan Electron Optical Laboratory Company, Limited) with an x-ray fluorescence spectroscopy attachment (Canberra Industries) for elemental analysis of the surfaces.

The concentrations of Cd⁺² and Ga⁺³ in solution from dissolution of the electrodes were determined polarographically at a dropping mercury electrode using a PAR 170 electrochemical system. Standard solutions were prepared from cadmium chloride and gallium metal dissolved in sulfuric acid. The solutions were degassed with prepurified nitrogen gas and the gallium was diluted and buffered with a 1M NH₃/1M NH₄Cl solution.

Results

The polycrystalline TiO₂ coats obtained were all hard and durable. The number of cracks and holes which formed in these coatings depended upon several factors, including the nature of the substrate material, the substrate temperature during deposition, the rate of heating and cooling of the substrate, the thickness of the TiO₂ coats, the number of TiO₂ coats applied, and the method of doping the TiO₂.

N-type substrate/n-TiO₂/solution.—Durable, crack- and hole-free coats of TiO₂ were obtained on n-Si and n-InP (Fig. 2a) by performing the CVD at a substrate temperature of 500°-600°C. At this temperature the coats annealed without additional heating and cooling (17). The substrate was held at this temperature for several hours to give at least a partial conversion from the anatase to rutile structure, and hydrogen gas was then passed over the surface to reduce it. The sample was then allowed to cool slowly over a 24 hr period.

The current *vs.* potential (*i-E*) curve for the n-InP/TiO₂ electrode with the TiO₂ exposed to solution (Fig. 3a) showed a cathodic dark current characteristic of an n-type semiconductor and an anodic photocurrent due to the oxidation of water, with bubbles being given off at the electrode surface and approximately a 60 mV/pH change in the onset of photocurrent. The current *vs.* wavelength (*i-λ*) plot (Fig. 3b) showed that the photocurrent absorption spectrum for the n-InP/TiO₂ electrode was identical to that of TiO₂. After several hours of illumination at +0.5V, there was no change in the amount of photocurrent or in the *i-λ* plot. There was also no visual decomposition of the TiO₂ film or apparent dissolution of the InP. In Fig. 3, the results of an uncoated n-InP electrode are shown for comparison. Similar results were observed with the n-Si/TiO₂ electrode. The TiO₂ was crack- and hole-free with anodic photoeffects observed and bubbles evolved at the surface only for λ < 400 nm (3.1 eV).

Crack-free TiO₂ coats were never obtained on n-CdS, even after repeated attempts using different conditions, as discussed above. The best coats were obtained by CVD at 600°C as before, but with reduction in high vacuum at 600°C. The electron micrographs are shown in Fig. 2b. With fast heating and cooling processes, there were at least ten times as many cracks. The *i-λ* curve, Fig. 4a, showed a large peak at about 480 nm due to the absorption of CdS with the current increasing with subsequent scans. The small current at about 350 nm, due to the excitation of TiO₂, decreased with time as the TiO₂ film deteriorated, as shown in Fig. 2c. The current *vs.* time curve, Fig. 4b, showed that the anodic photocurrent of pure CdS decreased, probably because of the formation of sulfur on the surface. With a TiO₂ film, the current increased with time, corresponding to the breakup of the TiO₂ film; the final current was limited by the sulfur buildup. Even for the portions of the TiO₂ that do not flake off, a sulfur layer can be seen to underlie the remaining and still durable TiO₂ film. Analysis of the solution, after passage of an anodic photocurrent for a given time, showed about 1% less Cd⁺² from the dissolution of CdS with TiO₂ on the surface as compared to CdS without TiO₂. Bubbles were not seen on the surface because of the small amounts of current going to the oxidation of water.

Crack- and hole-free coats were also not obtained on n-GaAs and n-GaP. Similar *i-λ* plots to those of n-CdS/TiO₂ were obtained with an absorption peak at about 350 nm, and a photocurrent which decreased with time. However, the substrate absorption peak currents increased with time because of the soluble products of dissolution. Bubbles were evolved at the electrode surface until a visible deterioration of the TiO₂ film was evident and solution analysis confirmed the presence of gallium.

P-type substrate/n-TiO₂/solution.—To examine further the band structure and possibilities for electron
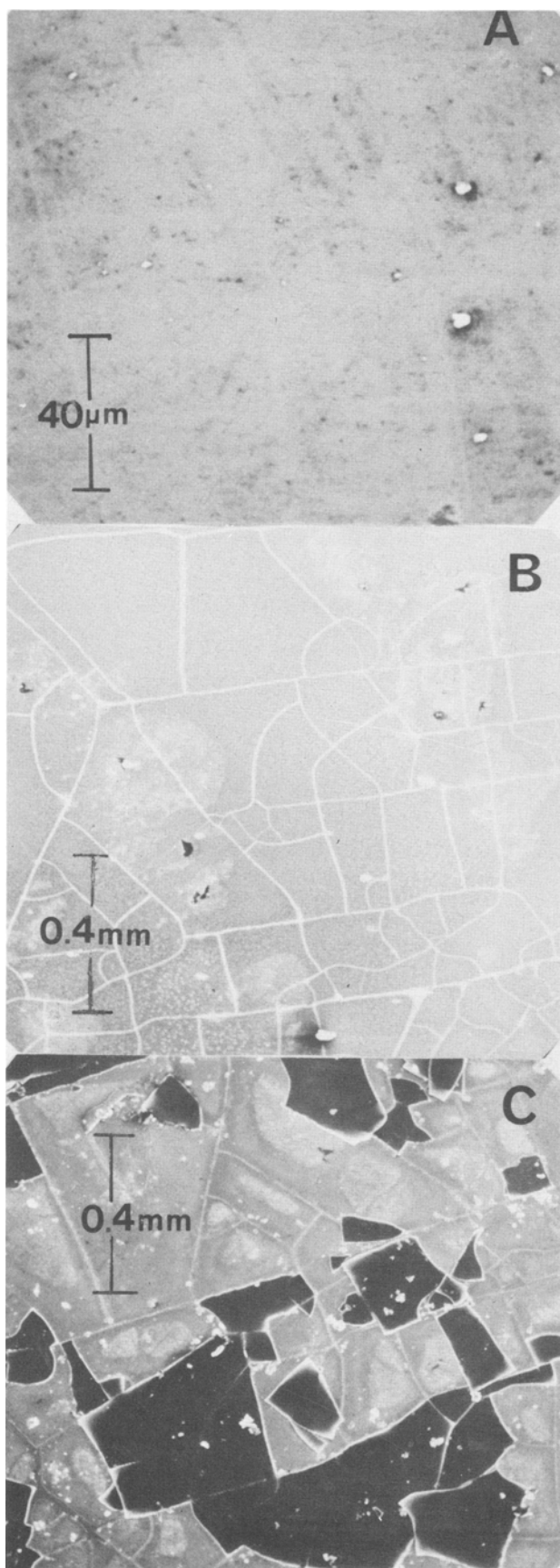
Fig. 2. (a) High contrast electron micrograph of n-Si with TiO_2 on the surface. The white spots are mounds of TiO_2 and the dark spots are shadows. (b) Electron micrograph of the n-CdS/TiO_2 electrode before use. The surface is covered with TiO_2 and the cracks are less than 10,000Å wide. (c) Electron micrograph of n-CdS/TiO_2 in (b) after the passage of current and dissolution of CdS. The dark areas are TiO_2 and light areas are CdS with sulfur in the cracks.
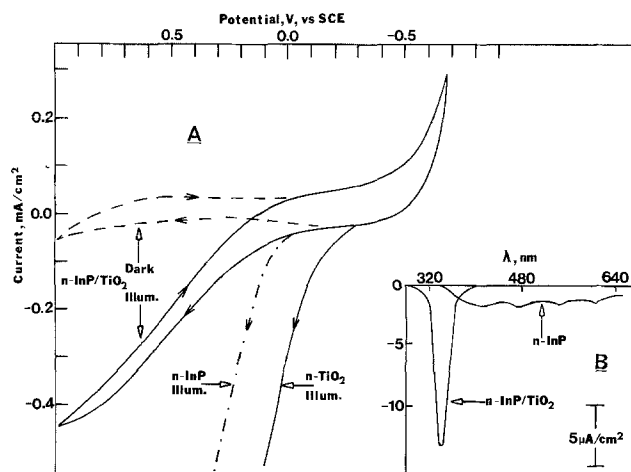

Fig. 3. (a) Current vs. potential for the n-InP/TiO_2 electrode in 0.5M Na_2SO_4, both in the dark and illuminated. The photocurrents of n-InP and n-TiO_2 are shown for comparison. (b) Current vs. wavelength for n-InP/TiO_2 and n-InP at +0.5V vs. SCE in 0.5M Na_2SO_4 (uncorrected for lamp intensity-monochromator spectral variations).
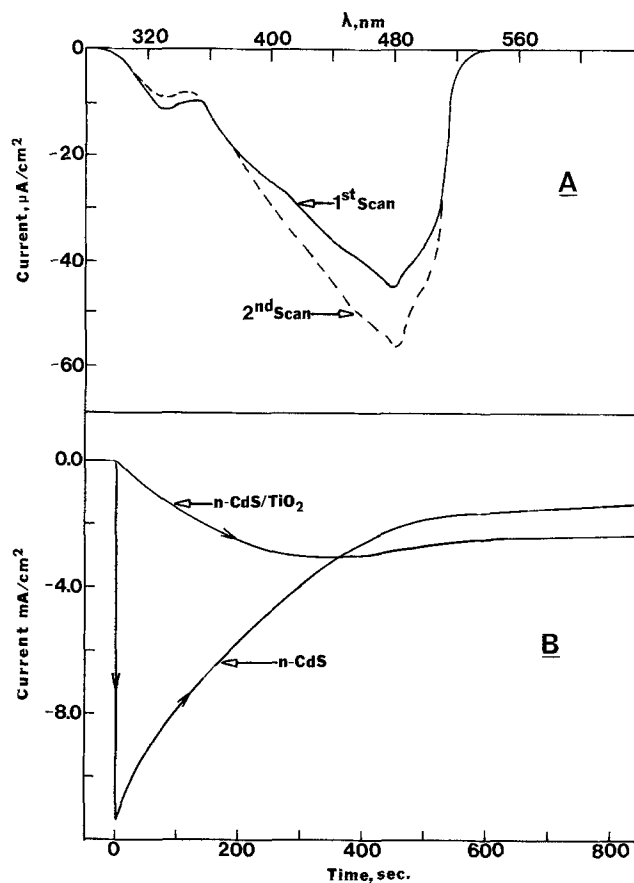

Fig. 4. (a) Current vs. wavelength for n-CdS/TiO_2 in 0.5M Na_2SO_4 at +0.5V (uncorrected for lamp intensity-monochromator spectral variations); (b) current vs. time for n-CdS/TiO_2 and n-CdS illuminated with white light in 0.5M Na_2SO_4 at +0.5V vs. SCE.

and hole transfer through the TiO_2, p-type materials were used as the substrates. This, in effect, gives holes in the substrate which are available for possible electron transfer to the solution without illumination.

Crack-free and stable coats of TiO_2 were obtained on p-Si and p-GaAs by the same procedure as described for n-Si and n-InP. The *i-E* curve of p-Si/TiO_2 (Fig. 5a) can be divided into three regions as indicated.
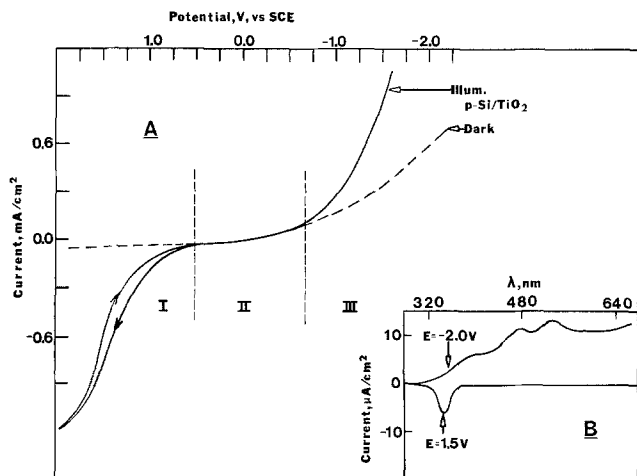
Fig. 5. (a) Current *vs.* potential for p-Si/TiO$_2$ in the dark and illuminated in 0.5*M* Na$_2$SO$_4$; (b) current *vs.* wavelength for p-Si/TiO$_2$ in 0.5*M* Na$_2$SO$_4$ at +1.5V and −2.0V *vs.* SCE (uncorrected for lamp intensity-monochromator spectral variations).

Significant photocurrents occurred in regions I and III. The anodic photocurrent in region I (Fig. 5b) is due to electron/hole pair formation in the TiO$_2$ resulting in the oxidation of water with bubbles evolved at the electrode surface. The potential for the onset of anodic photocurrent was pH dependent (*i.e.*, 60 mV/pH). In region III, the cathodic photocurrent can be attributed to the reduction of H$^+$ by photoexcitation of the p-silicon with again approximately a 60 mV/pH change in the onset of cathodic photocurrent. After several hours of illumination, there was no change in the cathodic or anodic photocurrents, nor was there a change in the *i*-λ curves. The same characteristic three regions were obtained on p-GaAs/TiO$_2$, but with the onset of significant anodic photocurrent at about +0.2V and significant cathodic photocurrent at about −0.7V in 0.5*M* Na$_2$SO$_4$.

i-V curves.—To investigate the TiO$_2$-substrate heterojunction, the current-voltage (*i-V*) curves on the solid-state junctions alone were taken by applying the indicated voltage to the front TiO$_2$ contact with respect to the rear substrate contact (Fig. 6a). Similar results were obtained for the various other substrate materials used. These results are discussed in the next section.
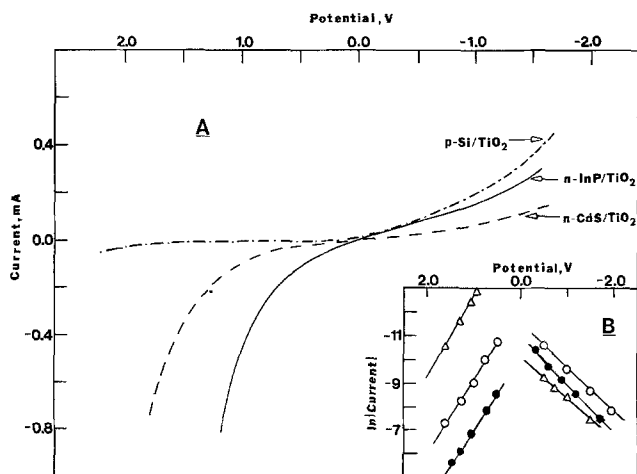

Fig. 6. (a) Current *vs.* voltage across the heterojunctions: p-Si/TiO$_2$, n-InP/TiO$_2$, n-CdS/TiO$_2$. (b) Natural log of current *vs.* voltage: △ = p-Si/TiO$_2$, ○ = n-CdS/TiO$_2$, ● = n-InP/TiO$_2$.

Discussion

The results for n-InP and n-Si with TiO$_2$ on the surface show the photo-oxidation of water can only be accomplished by the excitation of an electron-hole pair in the TiO$_2$. The creation of a hole in the n-type substrate has no mechanism for transfer through the TiO$_2$ to the solution. The observed 60 mV/pH shift in the onset of photocurrent at the TiO$_2$-covered substrates reflects the shift in the surface hydroxide equilibrium brought about by pH changes, as discussed by Honda and co-workers (19) for TiO$_2$ single crystals. The small bandgap substrates are stabilized with completely reproducible results from day to day and with no passivation or change in behavior.

Although the results are inconclusive, it appears that a similar lack of hole transfer through the film occurs in the other n-type semiconductors used in this study. The dissolution processes which occur at n-GaP, n-CdS, and n-GaAs appear to be taking place through the cracks in the TiO$_2$ (Fig. 2b and 2c). The increase in anodic photocurrent with time correlates with the removal of TiO$_2$ from the surface, just as the decrease in current at λ = 350 nm and the decrease in evolution of bubbles correlates with the removal of TiO$_2$.

The results for p-GaAs and p-Si with TiO$_2$ on the surface (Fig. 5) also show that the anodic photo-oxidation of water, region I, is due only to the excitation of an electron-hole pair in the TiO$_2$. The small dark current, even at +2.0V, shows that holes are not transferred through the TiO$_2$ to the solution. The cathodic photocurrent, region III of Fig. 5, is due to the reduction of hydrogen ion by photoexcited electrons in the conduction band of the substrate material that transfer through the TiO$_2$ to the solution. The potential at which this takes place is even more negative than that required for the reduction of hydrogen ion at a platinum electrode in the same solution. Region II of Fig. 5 lies between these two extreme regions with very small anodic photocurrents due to the excitation of TiO$_2$ and very small cathodic photocurrents from the excitation of the substrate. The substrates were again stable with no change in behavior with time.

The nature of the heterojunction produced between the small bandgap substrate and TiO$_2$ can be represented to a first approximation by simple band structures, shown in Fig. 7 (20). This neglects such things as the change in work function of TiO$_2$ with interaction with the water (21) or air pressure (16). This also does not consider the possibility of intermediate compounds being formed at the junction creating additional barriers, or the presence of surface states. The potential barrier at the n-n heterojunction arises from the mismatch of the conduction bands and Fermi levels. If the energies of the conduction bands and Fermi levels of the n-substrate and TiO$_2$ were equal with an ideal junction, there would be no barrier to the majority carriers (22). This model is qualitatively confirmed by the results in Fig. 6a, where the current varies with the exponential of the barrier potential, which changes in proportion to the applied potential. This is demonstrated in Fig. 6b by the linearity of the ln *i vs. V* plot. Therefore, because of the higher barrier for an electron to go from the TiO$_2$ to the n-type substrate, the conduction band of the substrate is higher than that of the TiO$_2$. The valence band of the TiO$_2$ must then lie far below that of the substrate. Therefore, a hole in the valence band of the substrate cannot travel downhill to the TiO$_2$ valence band without extreme band bending even if the nonidealities in the heterojunction, as mentioned above, are considered. It might be possible for hole transfer to occur through an intermediate level located in the bandgap region of the TiO$_2$ (6). However, no evidence for this type of transfer was found in these studies.

When the electrodes are used in solution, there are two junctions to be considered: the substrate/TiO$_2$ heterojunction and the TiO$_2$/solution interface. At equi-
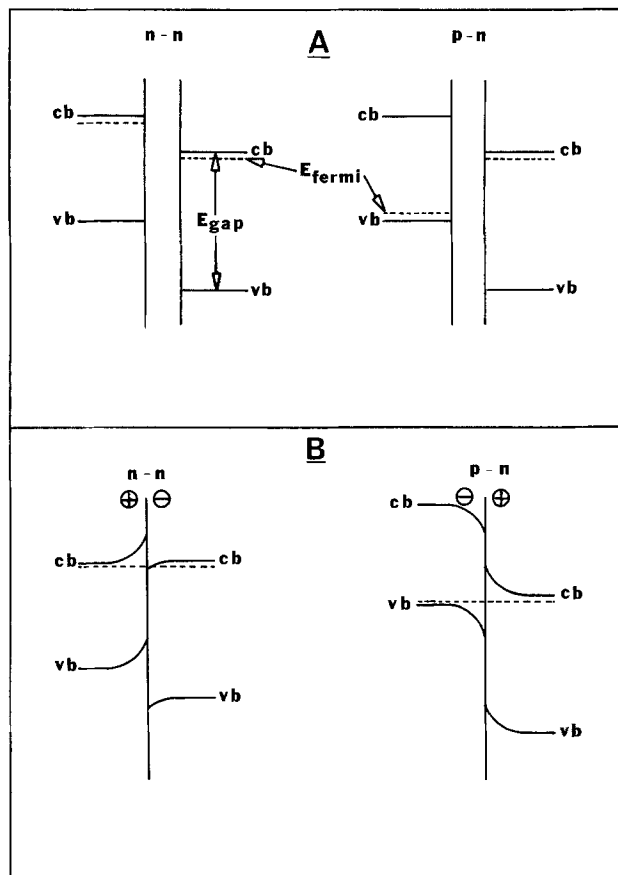
Fig. 7. Example of a n-n heterojunction and a p-n heterojunction (a) before contact, (b) after contact with the resulting band bending and charge separation.

librium, all Fermi levels must be equal. When a potential, ΔE, is applied to the electrode with respect to the solution and current flows, the position of the TiO_2 Fermi level is determined by the relative barriers at the two junctions (22). Assuming that the rate-determining step of the reaction at the TiO_2/solution interface is first order in concentration of holes or electrons at the surface, the current will depend not only upon the band bending of the TiO_2 at the solution interface but also upon the band bending of the substrate and TiO_2 at the heterojunction. A given current corresponds to a unique band-bending situation at both junctions. If a change in pH affects the potential drop between the electrode surface and solution, then the applied potential must be changed an equal amount to obtain the same band-bending situation and current. This explains the observed 60 mV/pH shift in onset of photocurrent.

Conclusion

Protective films of TiO_2 can be obtained by CVD on some semiconductor substrates without cracks. However, when cracks are present, dissolution of the substrate material can occur, with photocurrents caused by substrate dissolution at absorption wavelengths of the substrate. There does not appear to be any advantage in depositing TiO_2 on the n-type substrates used in this work, compared to the photo-oxidation of water over a CVD TiO_2 electrode itself, because of the inability to transfer holes from the substrate through the TiO_2. The use of p-type substrates coated with n-TiO_2 as photocathodes is limited by the band-bending requirements at the junctions and the barrier potential which must be overcome at the heterojunction, so that the required "negative overpotentials" for useful conversion of light energy do not occur.

Acknowledgments

REFERENCES

1. H. Gerischer and W. Mindt, *Electrochim. Acta,* **13,** 1329 (1968).
2. H. Gerischer, in "Physical Chemistry: An Advanced Treatise," Vol. 9A, H. Eyring, D. Henderson, and W. Jost, Editors, Academic Press, New York (1970).
3. D. Laser and A. J. Bard, *J. Phys. Chem.,* **80,** 459 (1976).
4. V. A. Myamlin and Y. U. Pleskov, "Electrochemistry of Semiconductors," Plenum Press, New York (1967).
5. Y. Nakato, T. Ohnishi, and H. Tsubomura, *Chem. Lett.,* **1975,** 883.
6. S. N. Frank and A. J. Bard, *J. Am. Chem. Soc.,* **97,** 7427 (1975).
7. A. B. Ellis, S. W. Kaiser, and M. S. Wrighton, *ibid.,* **98,** 1635 (1976).
8. S. R. Morrison, *Surf. Sci.,* **15,** 363 (1969).
9. K. H. Beckmann and R. Memming, *This Journal,* **116,** 368 (1969).
10. T. Watanabe, A. Fujishima, and K. Honda, *Bull. Chem. Soc. Jpn.,* **49,** 355 (1976).
11. M. S. Wrighton, D. S. Ginley, P. T. Wolczanski, A. B. Ellis, D. L. Morse, and A. Linz, *Proc. Nat. Acad. Sci. U.S.A.,* **72,** 1518 (1975).
12. F. Möllers and R. Memming, *Ber. Bunsenges. Phys. Chem.,* **76,** 469 (1972).
13. J. O'M. Bockris and K. Uosaki, Paper 14 (Inorganic Section) presented at the American Chemical Society Meeting, New York, New York, April 1976.
14. D. Laser, Unpublished results, 1975.
15. A. L. Milnes and D. L. Feucht, "Heterojunctions and Metal-Semiconductor Junctions," Academic Press, New York (1972).
16. T. Iida and H. Nozaki, *Bull. Chem. Soc. Jpn.,* **42,** 243 (1969).
17. K. Hardee and A. J. Bard, *This Journal,* **122,** 739 (1975).
18. R. K. Willardson and A. C. Beer, Editors, "Semiconductors and Semimetals," Vol. 7A, p. 65, Academic Press, New York (1971).
19. T. Watanabe, A. Fujishima, and K. Honda, *Chem. Lett.,* **1974,** 897.
20. T. L. Tansley, in "Semiconductors and Semimetals," Vol. 7A, R. K. Willardson and A. C. Beer, Editors, Academic Press, New York (1971).
21. E. N. Figurouskaya, *Kinet. Katal.,* **10,** 453 (1969).
22. R. M. Walzer, Private communication.